DESCENDING MEDULLARY PROJECTIONS TO THE PHRENIC MOTONEURON POOL AFTER HIGH CERVICAL SPINAL HEMISECTION

By

MARCELLA ANGELIQUE COUTTS

A THESIS PRESENTED TO THE GRADUATE SCHOOL
OF THE UNIVERSITY OF FLORIDA IN PARTIAL FULFILLMENT
OF THE REQUIREMENTS FOR THE DEGREE OF
MASTER OF SCIENCE

UNIVERSITY OF FLORIDA

2008

To Dante. Thank you for all of the love and support.

ACKNOWLEDGMENTS

I would like to thank my mentor, Dr. Paul Reier, for all of his help. In addition, I would like to thank the members of the Reier lab: Dr. Michael Lane, Dr. Todd White, Kevin Siegel, and Barbara O'Steen, all of whom continually offered their support and guidance.

TABLE OF CONTENTS

LIST OF TABLES

LIST OF FIGURES

LIST OF ABBREVIATIONS

A5	A5 Noradrenaline Cells
ABC	Avidin-biotin Complex
CNS	Central Nervous System
CPP	Crossed Phrenic Phenomenon
CVL	Caudal Ventrolateral Reticular Nucleus
DAB	Diaminobenzidine
DPGi	Dorsal Paragigantocellular Nucleus
FG	Fluorogold
Gi	Gigantocellular Reticular Nucleus
GiA	Gigantocellular Reticular Nucleus, Alpha Part
GiV	Gigantocellular Reticular Nucleus, Ventral Part
i.p.	Intraperitoneal
IRt	Intermediate Reticular Nucleus
LTF	Long-term Facillitation
LTP	Long-term Potentiation
LPGi	Lateral Paragigantocellular Nucleus
MRt	Medial Reticular Formation
NGS	Normal Goat Serum
NSCISC	National Spinal Cord Injury Statistical Center
PBS	Phosphate Buffered Saline
pfu	Plaque Forming Units
PhMN	Phrenic Motoneuron
PK15	Porcine Kidney
PRV	Pseudorabies Virus

REM	Rapid Eye Movement
RMg	Raphe Magnus Nucleus
RO	Raphe Obscurus Nucleus
RPa	Raphe Pallidus Nucleus
RVL	Rostroventrolateral Reticular Nucleus
rVRG	Rostral Ventral Respiratory Group
SCI	Spinal Cord Injury
s.q	Subcutaneous
SubC	Subcoeruleus Nucleus
VRC	Ventral Respiratory Column
WGA-HRP	Wheatgerm Agglutinin Conjugated to Horseradish Peroxidas

Abstract of Thesis Presented to the Graduate School
of the University of Florida in Partial Fulfillment of the
Requirements for the Degree of Master of Science

DESCENDING MEDULLARY PROJECTIONS TO THE PHRENIC MOTONEURON POOL AFTER HIGH CERVICAL SPINAL HEMISECTION

By

Marcella Angelique Coutts

August 2008

Chair: Paul J. Reier
Major: Medical Sciences

Neuroplasticity, which is an experience-dependent change in neural control, can occur in response to many stimuli and via many mechanisms throughout the peripheral and central nervous systems. Specifically, the respiratory system exhibits a remarkable capacity for plasticity-related changes. One extensively documented instance of respiratory neuroplasticity is the crossed phrenic phenomenon (CPP), which typically occurs after a high cervical spinal cord injury (SCI). The CPP involves the activation of a previously latent synaptic pathway that crosses the spinal midline to restore some activity to the phrenic motoneurons (PhMNs), which are denervated by SCI. Although much progress has been made in identifying the neural substrate that underlies the CPP, the current understanding of this instance of respiratory neuroplasticity is far from complete. In fact, few studies have examined the CPP and the neurons which drive diaphragm motor function at the level of the brainstem. Accordingly, the present study compares the phrenic-associated brainstem labeling that is observed when pseudorabies virus (PRV), a retrograde transneuronal tracer, is topically applied to the diaphragm in normal and C2-hemisected rats. It was found that the medial reticular formation (MRt) exhibits dominant connectivity to the PhMN pool both in the normal and injured animal. In a number of

species the MRt is involved in various behaviors which require alterations in breathing. Therefore, the function, connectivity, and relative stability of these cells after cervical hemisection suggests that they may be influential in modulating phrenic function both pre and post- injury.

CHAPTER 1
INTRODUCTION

Overview of Neuroplasticity

The term plasticity or neuroplasticity refers to a lasting change in a given neural control system as a result of prior experiences. The capacity for plasticity is inherent in the nervous system and can be manifested in response to numerous experiences or stimuli, including injury, disease, or aging (Mitchell and Johnson, 2003; Lane et al., 2008a; Nudo, 2007).

Plasticity can occur at numerous levels within a neuronal circuit by a variety of methods. For instance, changes in the activity level of a synapse can alter the subsequent efficacy of synaptic transmission. One example is known as long-term potentiation (LTP), whereby high frequency stimulation of a neuron results in a prolonged increase in synaptic efficacy. Other possible morphological alterations include changes in the size or shape of neurons and their processes (Mitchell and Johnson, 2003).

In addition to changes at the cellular level, plasticity-related changes can also occur at higher organizational levels, possibly affecting entire neural networks. For instance, experience-dependent changes are known to occur in the concentration or profile of neurotransmitters that modulate entire neural systems. Plasticity can also be manifested as the emergence of novel characteristics of neural networks. For instance, after a plasticity-inducing experience, a network of neurons could exhibit greater synchrony in their firing pattern (Mitchell and Johnson, 2003). Thus, neuroplasticity is the nervous system's remarkable ability to adapt in response to novel stimuli.

Models of Respiratory Neuroplasticity

Although the entire nervous system has the potential for plasticity, the focus of the present work is on the respiratory system. Numerous experiences, such as hypoxia or oxygen

deprivation, have been found to induce plasticity in the neural systems which control respiration (Mitchell and Johnson, 2003; Goshgarian, 2003). For instance, intermittent exposure to hypoxic conditions causes a sustained increase in the firing rates of the phrenic motoneurons (PhMNs), which control diaphragm contractions during inspiration. This increase in respiratory motor output is an instance of neuroplasticity referred to as long-term facilitation (LTF) and results in a prolonged increase in breathing frequency and tidal volume (i.e., the volume inspired or expired per breath) (Baker and Mitchell, 2000).

Another activity that can induce neuroplasticity in the respiratory motor system is exercise. In particular, repeated exercise that consistently induces hypercapnia (i.e., increased levels of carbon dioxide in the blood) results in a sustained ability to increase ventilation during subsequent exercise. This phenomenon is known as long-term modulation (Martin and Mitchell, 1993) and has been shown to occur via serotonin-dependent mechanisms (Johnson and Mitchell, 2001).

Many other instances of respiratory neuroplasticity have been documented. However, the most commonly investigated instance of respiratory neuroplasticity that has been observed across a variety of species is known as the crossed phrenic phenomenon (CPP) (Goshgarian, 2003). As will be discussed in more detail below, the CPP refers to a recovery of activity to denervated PhMNs via the activation of previously latent synaptic pathways that cross the spinal midline (Goshgarian, 2003; Johnson and Mitchell, 2001). This mechanism of plasticity has been demonstrated experimentally by a lateral spinal cord hemisection above the third cervical level. Thus, before discussing the CPP in detail, it is necessary to explain why a high cervical SCI represents a clinically relevant model for respiratory neuroplasticity.

High Cervical Spinal Cord Injury as a Clinically Relevant Model of Injury-Induced Respiratory Neuroplasticity

Traumatic injury to the cervical spinal cord is the most common type of SCI and accounts for approximately 52.4 % of all reported cases of SCI (National Spinal Cord Injury Statistical Center (NSCISC), 2006). An injury to one of the eight segments of the cervical spinal cord can produce a variety of life-threatening functional deficits which may include tetraplegia, sensory and motor losses below the level of injury, cardiovascular problems, autonomic dysreflexia, impaired bladder and bowel control, and respiratory dysfunction. Due to the broad range of morbidity that is associated with injury to the cervical spinal cord, it is no surprise that the highest levels of medical expenditures for all types of SCI are linked to this type of injury (NSCISC, 2006). However, even with the multitude of symptoms associated with cervical SCI, it is the respiratory complications that are most debilitating and potentially life-threatening. In fact, respiratory dysfunction and associated secondary complications represent the leading cause of morbidity and mortality after SCI at any level (Brown et al., 2006; Jackson and Groomes, 1994; NSCISC, 2006).

This comes as no surprise, since the neuronal connections that control inspiration are severed by a high cervical SCI. As the PhMNs that control the contraction of the diaphragm (i.e., the primary muscle of inspiration) are located at C3-C5, individuals who sustain a high (i.e., rostral to C3-4) cervical SCI may experience hemidiaphragm paresis ipsilateral to the injury due to denervation of the PhMNs. Consequently, such an injury is characterized by severe respiratory insufficiency and the development of a compensatory rapid, shallow breathing pattern, often causing patients to require the support of mechanical ventilation (Brown et al., 2006).

However, despite the severe consequences of denervation associated with this type of injury, there is the potential for neuroplasticity and functional recovery in this system via the

CPP. Although much of the evidence documenting the CPP after high cervical SCI has been demonstrated in animal models, it is tempting to speculate that some respiratory neuroplasticity may occur in humans after SCI. In fact, human SCI patients have shown some restoration of descending neural drive to the diaphragm that allows for modest recovery of respiratory function (Brown et al., 2006). Therefore, studying the mechanism underlying the CPP may lead to a better understanding of how respiratory neuroplasticity can be exploited clinically in SCI patients. For these reasons, a thorough understanding of the mechanisms related to neuroplasticity and recovery of respiratory functioning after high cervical SCI via the CPP is of utmost importance.

Current Understanding of the Neural Circuitry Associated with the Crossed Phrenic Phenomenon

One of the first historical accounts of the CPP and the associated restoration of respiratory function was described by Porter (1895). In Porter's study, hemisections were performed rostral to the level of the PhMN pool in dogs and rabbits to induce paralysis in the ipsilateral hemidiaphragm. It was observed post-hemisection that subsequent transection of the phrenic nerve (i.e., a phrenicotomy) contralateral to injury resulted in the restoration of some diaphragm function on the side of injury. Since then, the CPP has been demonstrated in a variety of species after C2 hemisection of the spinal cord (Goshgarian, 2003; Lane et al., 2008a).

In the rat, PhMNs receive descending inspiratory drive via axons originating from neurons in a region of the medulla called the ventral respiratory column (VRC) or rostral ventral respiratory group (rVRG) (Goshgarian, 2003). Previous neuroanatomical studies have shown that rVRG projections on either side of the spinal cord descend from cells on both sides of the medulla via a brainstem decussation and terminate monosynaptically on PhMNs (Ellenberger et al., 1990; Moreno et al, 1992). These PhMNs control diaphragm activity via the phrenic nerves.

Collectively, this neuronal network that controls inspiration is known as the "phrenic respiratory circuit."

After C2 hemisection, the descending medullary fibers in the phrenic respiratory circuit are interrupted. As a result, the ipsilateral PhMNs are denervated and become functionally silent, causing hemiparalysis of the ipsilateral diaphragm. However, despite this denervation, some functional recovery of ipsilateral diaphragm function and PhMN activity occurs after injury. Such recovery has been credited to the CPP, which involves the activation of a previously latent pathway that originates from medullary bulbospinal axons that cross the spinal midline at the level of the PhMNs to terminate monosynaptically on ipsilateral PhMNs (Goshgarian, 2003; Goshgarian et al., 1991; Moreno et al., 1992). The CPP can evolve either spontaneously (Fuller et al., 2006; Fuller et al., 2003; Golder and Mitchell, 2005; Golder et al., 2001b; Nantwi et al., 1999) or be induced under controlled, terminal neurophysiological conditions by subsequent transection of the contralateral phrenic nerve (Porter, 1895; Goshgarian, 2003).

Numerous studies have attempted to further define the neuroanatomical basis for the CPP in the rat. However, these studies have largely focused on the phrenic circuit at the level of the PhMN pool (Lane et al., 2008b; Goshgarian et al., 1991). Even the few studies which have ventured to look at the brainstem after hemisection have limited their examination of supraspinal phrenic projections involved in the CPP to the VRC (Boulenguez et al., 2007; Moreno et al., 1992). In contrast, only one study has attempted to examine the complete profile of brainstem neurons involved in the phrenic respiratory circuit; however this study was restricted to uninjured animals and did not examine the potential for neuroplasticity in the circuit after injury (Dobbins and Feldman, 1994). Therefore, to construct a more complete picture of the mechanism behind the CPP in the respiratory system, the experiments performed in this thesis

will examine the entire profile of pre-phrenic brainstem neurons involved in the CPP in the rat after a C2 hemisection and in the process will also reexamine the normal supraspinal phrenic respiratory circuit.

Previous Studies on Brainstem Phrenic Circuitry

As mentioned above, there have been very few neuroanatomical studies examining the changes in supraspinal projections to the phrenic nucleus after C2 hemisection. In one such study, Boulenguez et al. (2007) attempted to quantify the extent of projections from the rVRG that cross at the level of the PhMNs and are likely to be involved in the CPP. In that study, injections of fluorogold (FG), a monosynaptic retrograde tracer, were made directly into the spinal cord below a C2 hemisection (at C3-C4). Because injections were made below the hemisection into the denervated PhMN pool, the labeled neurons in the brainstem could only become labeled if their axons crossed the spinal midline. Boulenguez showed that, when compared to control animals, injured animals showed reduced labeling bilaterally in the rVRG and that labeling was particularly sparse on the side ipsilateral to injury. Comparison of FG-labeled rVRG neuron counts in injured versus control animals showed that after hemisection, labeling was reduced to only 23 % ipsilaterally and 36 % contralaterally of the labeling observed in control animals. The authors felt that this subpopulation of cells that cross the spinal midline represented the neuroanatomical substrate for the CPP. Although this study examined supraspinal projections from the rVRG to PhMNs involved in the CPP, it failed to yield any information regarding the broader neuronal network which controls PhMN activity in the injured animal.

One other study has directly examined the brainstem neuronal network which controls PhMNs (Dobbins and Feldman, 1994). In that series of experiments, the authors injected the Bartha strain of Pseudorabies Virus (PRV) into phrenic nerves of normal animals. PRV-Bartha

has been repeatedly found to produce viral infections in an exclusively retrograde direction (i.e., from axon terminal to cell body) (Card et al., 1998). Thus, infection with this neurotropic virus resulted in very specific labeling of the PhMNs, thereby suggesting that the PRV-labeled cells in the brainstem were restricted to neurons in the phrenic respiratory circuit.

Also, PRV produces temporal waves of infection in a manner that is consistent with the pattern of innervation in a circuit (Lowey, 1998). Thus, because numerous regions of the brainstem showed labeling, it was evident that a widespread network of cells in the brainstem was responsible for motor control of the diaphragm. However, despite labeling in numerous brainstem regions, Dobbins and Feldman concluded that, because the largest quantity of PRV-positive neurons in any brainstem region known to be inspiratory were found in the region of the rVRG, monosynaptic projections from the rVRG must represent the dominant anatomical pathway to the PhMNs. Because that study focused exclusively on the brainstem regions involved in modulating PhMN excitability in the uninjured animal, it did not provide information on plasticity-related changes in the phrenic respiratory circuit via the CPP.

Overview of Thesis Study

The present study was designed to further examine the brainstem phrenic respiratory circuitry and the plasticity observed in this system after SCI using PRV-Bartha as a neuroanatomical tracer. Since previous studies of this circuit at the supraspinal level have not produced a complete picture of all of the brainstem areas with descending projections to PhMNs in the normal or injured case, it is important to quantify the distribution of brainstem neurons in this network in both control and injured animals. Moreover, because PRV has been found to travel in a time-dependent fashion across a multisynaptic circuit based on density of synaptic connections (when viral titer is held constant), neurons that show more synaptic connectivity to the region of application will show earlier infection (Card et al., 1999). Therefore, to provide

insight concerning the density of connectivity to PhMNs and to determine whether this connectivity is subject to changes after a C2 hemisection, it is also important to closely examine the time-course of PRV-labeling which occurs in this circuit. This information will expand the current understanding of the neural substrate and mechanisms of plasticity mediating the CPP.

Therefore, the objective of the present investigation was to compare phrenic-associated brainstem labeling patterns when PRV is topically applied to the diaphragm in normal rats and C2-hemisected rats. In addition, the aim of this study was to examine the differences in relative numbers of labeled cells in various brainstem areas throughout a time course after the PRV infection of uninjured animals to ascertain which brainstem areas most densely innervate the PhMNs and to determine whether these regions change after C2 hemisection.

CHAPTER 2
MATERIALS AND METHODS

Animals

Adult female Sprague-Dawley rats (250-300 g) were obtained from Harlan Scientific and subsequently housed at the University of Florida's McKnight Brain Institute Animal Care Facility. All surgical and animal care procedures were conducted under approval from the Institutional Animal Care and Use Committee at the University of Florida. A total of 17 animals were used in this study.

Pseudorabies Virus

PRV 152 was generously provided by Dr. David C. Bloom (University of Florida). This virus is a recombinant of the Bartha strain of PRV and has a viral titer of 8.0-9.9x10^8 pfu/ml. Biosafety Level II practices (U.S. Department of Health and Human Services, 1988) were employed in all phases of PRV usage. This virus was prepared by producing seed stocks on porcine kidney (PK15) cells which were obtained from the American Type Culture Collection. The PK15 cells were grown at 37°C, 5% CO2 with humidity in MEM Medium with Earl's salts (Invitrogen). These cells were supplemented with nonessential amino acids, 10% fetal bovine serum and antibiotics (250 U of penicillin/ml, 250 μg of streptomycin/ml). Viral stocks were then produced by infecting near confluent PK15 monolayers at a multiplicity of infection of 0.01. Once they exhibited a 100% cytopathic effect, the cells and medium were harvested and centrifuged at 16,000 x g for 40 min, then re-suspended in 1/100th of the original volume of medium, and subjected to two rounds of freeze-thaw. The stocks were subsequently aliquoted into 100 μl volumes and stored at -80°C. The aliquots were titrated for infectious virus on monolayers of PK15 by standard plaque assay under agarose.

Surgical Procedures

Anesthesia and Post-Operative Care

Surgical procedures were performed under aseptic conditions in a dedicated surgery room. For all surgical procedures, the animals were deeply anesthetized using injections of xylazine (0.15ml per animal, subcutaneous (s.q.)) and ketamine (1ml/kg body weight, intraperitoneal, (i.p.)). Once the necessary surgical procedure was completed, each animal received an injection of Yohimbine (0.2ml per animal, s.q.) to reverse the anesthesia and lactated ringers solution (5ml per animal, s.q.) to prevent dehydration. As the animals began to recover from anesthesia, they were given Buprenorphrine for analgesia (0.4ml of 0.3mg/ml, s.q.). The subsequent recovery of the animals was monitored over the next several days.

Spinal Cord Injury

For experiments involving spinal hemisection (n=4), an incision was made through the skin and underlying muscle which extended about one inch from the base of the skull. Subsequently, a laminectomy was performed to remove the second cervical vertebra (C2). A small dural incision was then made and a lateral C2 hemisection was performed by creating a cavity on the left side of the spinal cord with a microscalpel and aspiration using an angled, fine tipped glass pipette. The dura was closed with interrupted 10-0 sutures and covered with Durafilm. The muscle was sutured in layers with 4-0 Vicryl (polyglactin 910, synthetic absorbable sterile suture) and the skin was stapled closed with wound clips. Injured animals were then allowed to recover 2 weeks after the hemisection surgery, then perfused fixed to examine histology. Forty eight to sixty four hours prior to perfusion, all animals (injured or uninjured) also received surgery for neuroanatomical tracing.

Retrograde Neuroanatomical Tracing

Brainstem neurons premotor to PhMNs were labeled with PRV 152 in both uninjured (n=13) and C2-hemisected animals (n=4). An incision approximately one inch long was made through the skin and underlying muscle of each animal's ventral surface along the linea alba, starting from approximately the base of the sternum. Retractors were used to deflect the skin and muscle to gain access to the lower surface of the diaphragm. PRV 152 (40-50µl) was then topically applied with a paintbrush to the left hemi-diaphragm. The abdominal muscle was then sutured with Vicryl sutures and the skin was stapled closed with wound clips. The animals were left to recover for either 48 (n=4 uninjured), 56 (n=4 uninjured) or 64 (n=5 uninjured, n=4 injured) hours after application of the tracer, at which time they were sacrificed.

Perfusion and Tissue Sectioning

At the end of the experiment, each animal was given a lethal dose (0.4 ml per animal) of Beuthanasia (phenytoin and sodium pentabarbitone; minimum of 1ml/kg body weight, i.p.) Upon cessation of breathing, the chest cavity was opened and animals were intracardially perfused with 250 ml of 0.9% saline (with heparin and 0.2% sodium nitrite to prevent clotting) followed by 500 ml 4% paraformaldehyde (in 0.1M phosphate buffered saline (PBS)). Next, the brain and spinal cord were removed from each animal and post-fixed by immersion in 2% paraformaldehyde at 4º C until subsequent processing. Transverse brainstem sections and either transverse or longitudinal spinal cord sections were cut with a vibratome at a thickness of 40 µm. Sections were collected sequentially in welled plates containing 2% paraformaldehyde. These sections were stored at 4º C until subsequent immunohistochemical processing.

Immunohistochemistry

Sections were initially washed in PBS (0.1 M, three times for five minutes), then incubated in quenching solution (30% methanol, 0.6% hydrogen peroxide in 0.1M PBS, for one

hour) in order to reduce endogenous peroxidase activity. The tissue was then re-washed in PBS (0.1 M, three times for five minutes) and subsequently incubated in blocking solution (10% normal goat serum in 0.1M PBS, for one hour) to reduce background staining due to non-specific protein labeling. Sections were then incubated in a primary antibody (rabbit anti-PRV (Rb134), dilution 1: 10,000) overnight at 4º C. The following day the tissue was re-washed in PBS (0.1 M, three times for five minutes) and then incubated in a biotinylated secondary antibody (goat anti-rabbit, Jackson Immunocytochemicals, dilution 1:200) for two hours at room temperature. Once again, the tissue was washed in PBS (0.1 M, three times for five minutes) and then incubated for another 2 hours in an avidin-biotin complex (ABC, Elite Vectastain Kit, Vector Labs). Sections were then given another series of washes in PBS (0.1 M, three times for five minutes) and the antigen was visualized with diaminobenzidine (DAB, Sigma). The sections were rewashed with PBS (0.1 M, three times for five minutes) and then mounted on Fisher superfrost slides.

All slide-mounted brainstem sections were then counterstained with Cresyl Violet (CV) in order to distinguish cell types and regions of the brainstem. Slides were immersed in butanol (2 min) then xylene (2 min) and once again in butanol (3 min). Next the slides were submerged in 100%, 95%, 70%, and then 50% ethanol (each for 3 minutes). After this the slides were placed in distilled water (3 min) and then into the Cresyl Violet stain (2 min). After this the slides were dipped briefly in distilled water (3 times) then placed in 50%, 70%, and 95% ethanol (each for 20 seconds). Slides were subsequently immersed in differentiation solution (1% glacial acetic acid in 95% ethanol) and monitored until the sections reached the desired level of staining, at which time they were placed into 100% ethanol (1 min), butanol (3 Min), and xylene (2 min). After staining, the slides were coverslipped with Richard-Allen Mounting Medium. Tissue sections were examined using brightfield microscopy. Brightfield photographs were taken

digitally using a Zeiss AxioPhot microscope with an AxioCam HRc digital camera linked to a PC. Image contrast and exposure was subsequently corrected using Adobe Photoshop 6.0 (Adobe Systems, Inc.).

Quantitative Analyses

Using brightfield microscopy, PRV-positive neurons in the brainstem with visible nuclei were counted at 10x magnification in consecutive transverse brainstem sections from each animal. *The Rat Brain in Sterotaxic Coordinates* atlas was used to localize the specific regions of the brainstem where staining was observed (Paxinos and Watson, 1997). Counts were made using the physical dissector method (Coggeshall and Lekan, 1996; Guillery, 2002). That is, only cells with a visible nucleus were counted to reduce the likelihood of counting a single cell twice in consecutive sections.

Statistical Analyses of Data

Statistical analyses were conducted using the SigmaStat 3.5 software package on a Dell Computer. Statistical significance was set at $p<0.05$. Unless otherwise indicated, pooled data are presented as mean $\pm$ S.E.

CHAPTER 3
RESULTS

Pseudorabies Virus Infection of the Cervical Spinal Cord

To verify that PRV had produced reliable infections, the cervical spinal cords of all animals (n=17) were qualitatively examined for the presence of PRV-positive PhMNs ipsilateral to the side of tracer application (Figure 3-1). There was no evidence found of bilateral PhMN pool labeling at any survival interval in injured or control animals. The lack of such labeling suggests that diffusion of the tracer to the contralateral hemidaphragm was not likely to have occurred in any of the animals.

Labeling of PhMNs ipsilateral to the application of tracer was observed in all animals. Consistent with previous reports, examination of the cervical spinal cord sections revealed that the number of infected PhMNs appeared to increase as time post-PRV application increased (Lane et al., 2008b). Representative sections of the PhMN labeling with PRV can be seen in Figure 3-1. Moreover, the distribution and arrangement of these neurons was found to match previous descriptions of the PhMN pool in the rat (Lane et al., 2008b; Dobbins and Feldman, 1994; Goshgarian and Rafols, 1981). That is, the PhMN pool appeared in longitudinal sections of the cervical spinal cord as a tight column of neurons which tilted slightly from a lateral position in the ventromedial gray matter (at higher levels of the cervical spinal cord) to a more medial position (at lower levels of the cervical spinal cord) and extended rostro-caudally from approximately C3 to C6. Also, the column was made up of distinct clusters of several neurons separated from each other at regular intervals for the length of the PhMN pool. As in previous reports of PRV labeling in the phrenic respiratory circuit, second-order labeled interneurons were observed predominantly in Rexed laminae VII and X of the cervical spinal cord (Lane et al., 2008b; Dobbins and Feldman, 1994).

Quantitative Analysis of Brainstem Labeling in Uninjured Animals

At 48 hours after infection, very few neurons were labeled in the brainstem. At more delayed post-infection time points (i.e., 56 and 64 hours after PRV application), increased PRV labeling was observed in numerous areas of the brainstem. Qualitatively, there appeared to be considerable variability between animals in the total number of PRV-positive neurons observed in the brainstem at any given post-infection time (Table 3-3). This variability is consistent with that observed in other studies which have employed this method of PRV delivery (i.e., topically to the diaphragm) to study this circuit in the cervical spinal cord (Lane et al., 2008b). Despite apparent variability, it seemed that the areas of the brainstem which exhibited the most labeling were comparable across the animals examined.

No infected neurons were detected in the dorsal motor nucleus of the vagus in any animal at any post-infection survival interval examined. The lack of staining in this region verifies that the viral infection was specifically restricted to the phrenic respiratory circuit and that the topical application of the virus to the diaphragm did not result in the infection of abdominal organs, which has previously been shown to cause labeling in this brainstem region (Card et al., 1990; Yates et al., 1999). Moreover, no glial cell infection was seen in the brainstem at any post-infection interval. This indicates that supraspinal spread of the viral infection was not likely to have occurred due to lysis of cell bodies, thereby supporting the presumption that the course of viral infection in this study occurred predominantly in a transynaptic fashion (Card et al., 1993).

To circumvent variability in raw counts of PRV-positive medullary neurons, the data were first expressed as a proportion of total infected brainstem neurons in that animal (Tables 3-1 and 3-2). Next, to make comparisons between the brainstem labeling observed in uninjured and C2-hemisected animals at 64 hours post infection, regional neuronal counts were reported as a proportion of total brainstem labeling on each side of the brainstem (Table 3-4). This lateralized

normalization was done to account for the fact that, as it has been previously reported (Boulenguez et al., 2007), injured animals showed extremely attenuated cell-labeling on the side of the brainstem ipsilateral to injury (Table 3-3).

Quantitative Analyses at the 48 and 56 Hour Post-Infection Interval

At 48 hours after delivery of PRV to the left hemidiaphragm (n=4), there was virtually no labeling seen in the brainstem. However, at 56 hours after PRV infection (n=4) a greater number of cells became infected in the brainstem. In all of these animals labeling was seen in multiple brainstem regions. At this post-infection interval many of these regions contained sparse labeling that was often inconsistent between animals. Nonetheless, the areas of the brainstem which showed the most consistent labeling (across the animals within this group) and on average accounted for approximately 5% or more of the total PRV-infected neurons in the brainstem (the "most labeled areas") included the medial reticular formation (MRt), the rostroventrolateral reticular nucleus (RVL), the A5 Noradrenaline Cells (A5), the Intermediate reticular nucleus (IRt) and the raphe nuclei (RO and RPa). It is notable that the rVRG accounted for only 3.5% of total labeling at this time point and was therefore excluded from the statistical analyses. Moreover, PRV-infected neurons in the MRt nuclei accounted for the largest proportion of total brainstem labeling observed on both the left and right sides of the brainstem in all four animals examined. In particular, the LPGi region of the MRt accounted for the largest proportion of all gigantocellular labeling observed (Table 3-1 and Figure 3-4).

To determine if any significant differences existed in the proportion of labeling in the total brainstem among the most labeled areas, a one-way repeated measures Analysis of Variance (ANOVA) was conducted on these areas at the 56 hour post infection interval. Differences were found between groups ($F(4, 19) = 56.32$, $p<0.001$). Post-hoc analyses were conducted using the Holm-Sidak pairwise multiple comparison procedure. Specifically, the MRt contained a

significantly greater proportion of brainstem labeling than the Raphe (t = 12.33, p<0.001), the IRt (t = 12.20, p<0.001), the A5 (t=11.63, p<0.001), and the RVL/CVL (t=11.10, p<0.001) (Figure 3-3). No other significant differences were found.

Since the MRt was the only significantly different region, a one-way repeated measures ANOVA was conducted to determine if any differences in the proportion of labeling existed among the specific subdivisions of the MRt (the LPGi, GiA, Gi, and GiV). Differences were found between groups (F(3, 15) = 37.77, p<0.001). Post-hoc analyses were conducted to isolate where significant difference(s) occurred using the Holm-Sidak pairwise multiple comparison procedure. Specifically, the LPGi contained a significantly greater proportion of brainstem labeling than the GiV (t=9.25, p<0.001), the Gi (t=8.53, p<0.001), and the GiA (t=8.15, p<0.001) (Figure 3-4). No other significant differences were found.

Further analyses were conducted to determine if differences existed in the proportion of labeling between the left and right sides of the brainstem in either the MRt or the LPGi. The data in the MRt failed the assumption of normality, and so were analyzed with Wilcoxon's Signed Rank Test. There were no significant differences between the left (median 30.10) and the right (median 23.43) sides of the MRt, (W=-6.00, p=0.25). The data in the LPGi passed the assumption of normality, and so were analyzed with a paired-samples t-test. No differences were found between the left (M=24.64$\pm$5.16) and the right (M=17.57$\pm$2.77) sides of the LPGi (t=1.09, p=0.36).

Quantitative Analyses at the 64 Hour Post-Infection Interval

At 64 hours post-infection more brainstem neurons showed infection with PRV and greater consistency was seen in the pattern of labeling across animals. Specifically, all animals in this group (n=5) showed consistent labeling that, on average, accounted for approximately 5% or more of the total PRV-infected neurons in the brainstem in the MRt nuclei, RVL/CVL, raphe

nuclei (RO, RPa, raphe magnus (RMg)), A5, rVRG, and subcoeruleus nuclei (SubC). Despite the slightly more consistent labeling seen at this post-infection interval, there were still regions of the brainstem which contained sparse and/or inconsistent labeling between animals within this group. However, the MRt, and in particular the LPGi, persisted as the brainstem region which showed the greatest proportion of labeled cells in all animals on both sides of the brainstem (Table 3-2 and Figures 3-5 and 3-6). A representation of the typical labeling seen can be found in Figure 3-2.

For the 64 hour time point, the same analyses were conducted as those at the 56 hour time point. To determine if any significant differences existed in the proportion of labeling in the total brainstem among the most labeled areas, a one-way repeated measures ANOVA was conducted on these areas at the 64 hour post infection interval. Differences were found between groups ($F(4, 29) = 45.35$, $p<0.001$). Post-hoc analyses to isolate these differences were conducted using the Holm-Sidak pairwise multiple comparison procedure. Specifically, the MRt had a significantly greater proportion of brainstem labeling than the SubC ($t=12.35$, $p<0.001$), rVRG ($t=12.35$, $p<0.001$), A5 ($t=11.55$, $p<0.001$), Raphe ($t=11.16$, $p<0.001$), and RVL/CVL ($t=9.71$, $p<0.001$) (Figure 3-5). No other significant differences were found.

Since the MRt was the only region found to contain a significantly greater proportion of labeling, a one-way repeated measures ANOVA was conducted to determine if any differences existed among the specific regions of the MRt (the LPGi, GiA, Gi, DPGi, and GiV). Differences were found between groups ($F(4, 24) = 69.75$, $p<0.001$). Post-hoc analyses were conducted using the Holm-Sidak pairwise multiple comparison procedure. Specifically, the LPGi had a significantly greater proportion of brainstem labeling than the DPGi ($t=14.11$, $p<0.001$), Gi

(t=13.31, p<0.001), GiV (t=12.90, p<0.001), and GiA (t=12.11, p<0.001) (Figure 3-6). No other significant differences were found.

Further analyses were conducted to determine if differences existed in the proportion of labeling between the left and right sides of the brainstem in the both the MRt and the LPGi at the 64 hour time point. The data in the MRt passed the assumption of normality, and so were analyzed with a paired samples t-test. There were no significant differences between the left (M=24.12$\pm$1.02) and the right (M=18.25$\pm$2.18) sides of the MRt (t=2.32, p=0.08). The data in the LPGi also passed the assumption of normality, and so were analyzed with a paired-samples t-test. No differences were found between the left (M=16.96$\pm$1.39) and the right (M=14.47$\pm$2.07) sides of the LPGi (t=1.10, p=0.33).

Quantitative Analysis of Brainstem Labeling in Injured Animals

In all injured animals there was less total labeling on the left side of the brainstem (i.e., ipsilateral to hemisection) than on the right (Table 3-3). Analyses were conducted to determine if medullary labeling patterns were altered two-weeks after a C2 hemisection. To assess differences in the laterality of labeling, two separate ANOVAs were conducted: one for the left side of the brainstem and one for the right side of the brainstem.

First, for the left side, a two-way repeated measures ANOVA (injury level x brainstem region) was conducted. Although the data violated the assumption of normality, they passed the equal variance test. There were significant differences among brainstem regions (F(6, 62)=15.88, p<0.01), however there were no significant differences between injury conditions (F(1, 61)=1.37, p=0.28), nor was the interaction term significant (F(6, 62)=0.36, p=0.90). Post-hoc analyses were conducted with the Holm-Sidak pairwise multiple comparison procedure. Specifically, the MRt contained a significantly greater proportion of left-side labeling than the rVRG (t=7.80, p<.001), IRt (t=7.76, p<0.001), SubC (t=7.72, p<0.001), A5 (t=7.38, p=0.001),

RVL/CVL (t=6.85, p<0.001), and Raphe (t=5.93, p<0.001) (Table 3-4 and Figure 3-7). No other significant differences were found.

The second test, for the right side, was also a two-way repeated measures ANOVA (injury level x brainstem region). Although the data violated the assumption of normality, they passed the equal variance test. Again, there were significant differences among brainstem regions (F(6, 62)=41.36, p<0.001), however there were no significant differences between injury conditions (F(1, 62)=0.02, p=0.89), nor was the interaction term significant (F(6, 62)=1.02, p=0.43). Post-hoc analyses were conducted with the Holm-Sidak pairwise multiple comparison procedure. Specifically, the MRt contained a significantly greater proportion of right-side labeling than the IRt (t=12.83, p<0.001), SubC (t=12.78, p<0.001), rVRG (t=12.68, p<0.001), A5 (t=10.83, p<0.001), RVL/CVL (t=10.60, p<0.001), and Raphe (t=10.33, p<0.001) (Table 3-4 and Figure 3-8). No other significant differences were found.

A

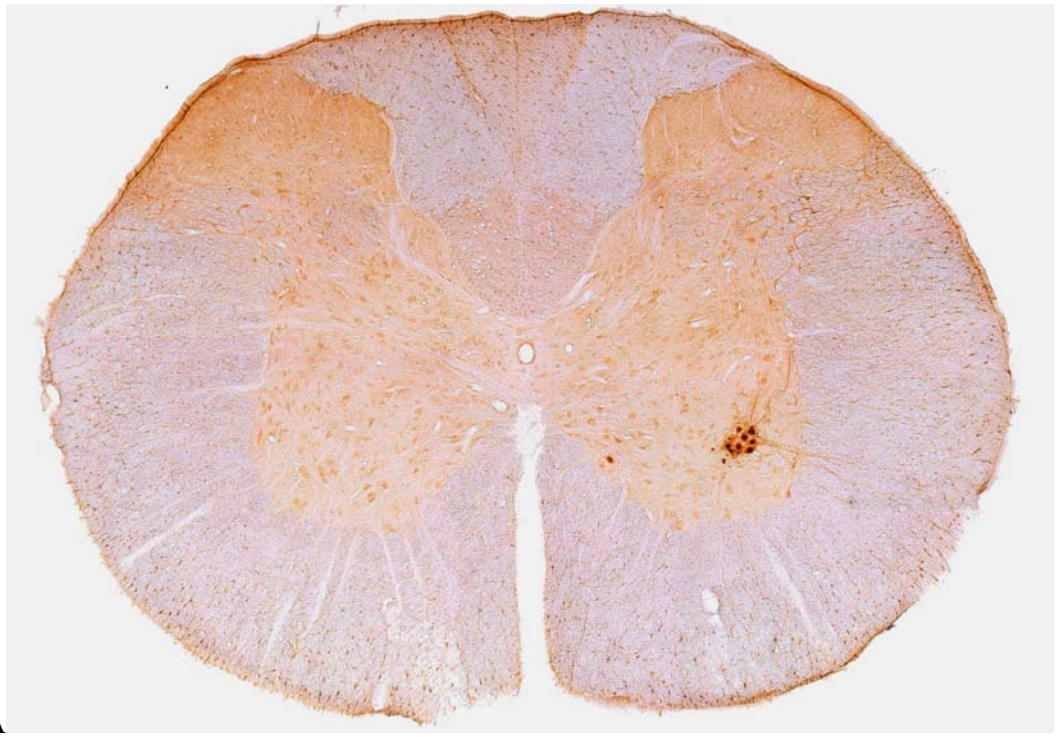

B

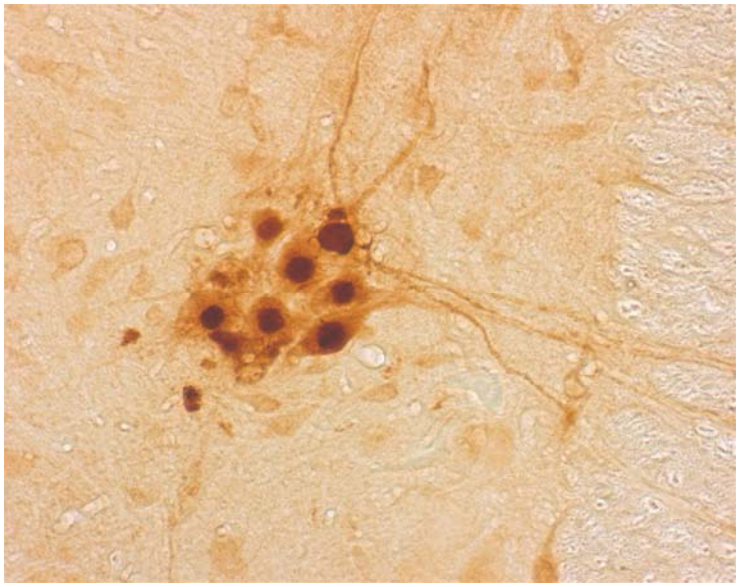

C

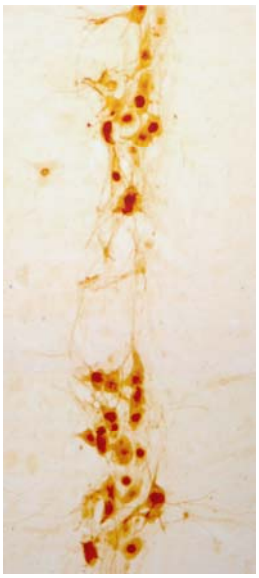

Figure 3-1: PRV-infected PhMNs are specifically labeled in the cervical spinal cord. A) A transverse spinal cord section that was obtained from approximately the C3 spinal level at 64 hours after PRV labeling of the left hemidiaphragm. B) Magnification of PRV-infected ipsilateral PhMNs in part A. C) A portion of the PhMN pool in a longitudinal spinal cord section at 64 hours after PRV labeling of the left hemidiaphragm (extending from rostral to caudal from top to bottom).

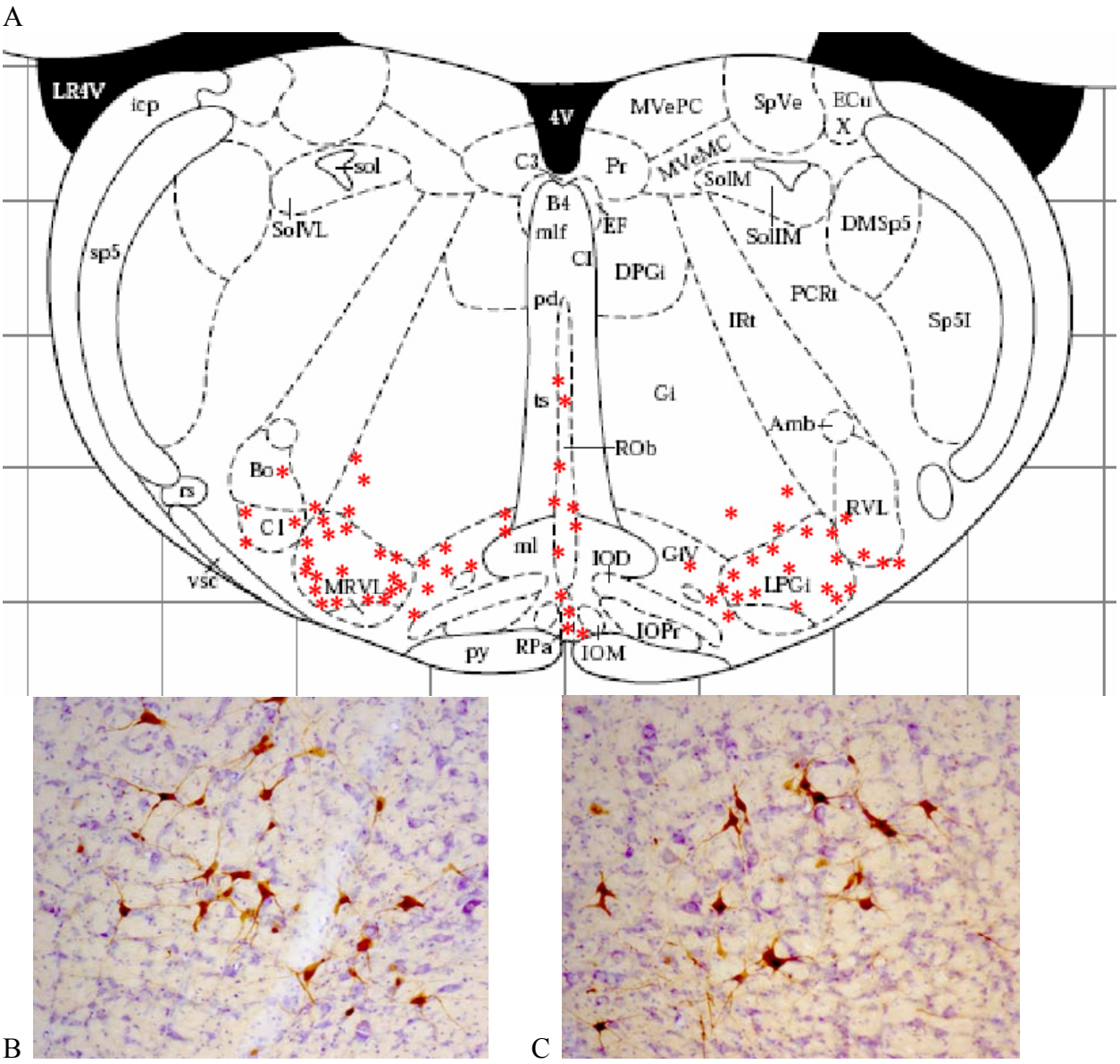

Figure 3-2: Brainstem labeling in the Medial Reticular Formation. A) Image of a transverse brainstem section from The Rat Brain in Sterotaxic Coordinates by Paxinos and Watson (1997). Red asterisks indicate PRV-positive neurons seen in four consecutive 40 µm brainstem sections at 64 hours post-infection. B) PRV-positive LPGi neurons on the Left side of the brainstem at 64 hours post-infection. C) PRV-positive LPGi neurons on the Right side of the brainstem at 64 hours post-infection.

Table 3-1: Percentage of total labeling in brainstem in each region at 56 hours

	Region	Mean	SE
Overall brainstem	MRt	56.28	4.33
	RVL/CVL	10.05	2.50
	A5	7.84	2.46
	IRt	5.48	2.60
	Raphe	4.95	0.83
Regions of MRt	LPGi	42.21	5.15
	GiA	6.81	1.54
	Gi	5.20	1.58
	GiV	2.06	1.24

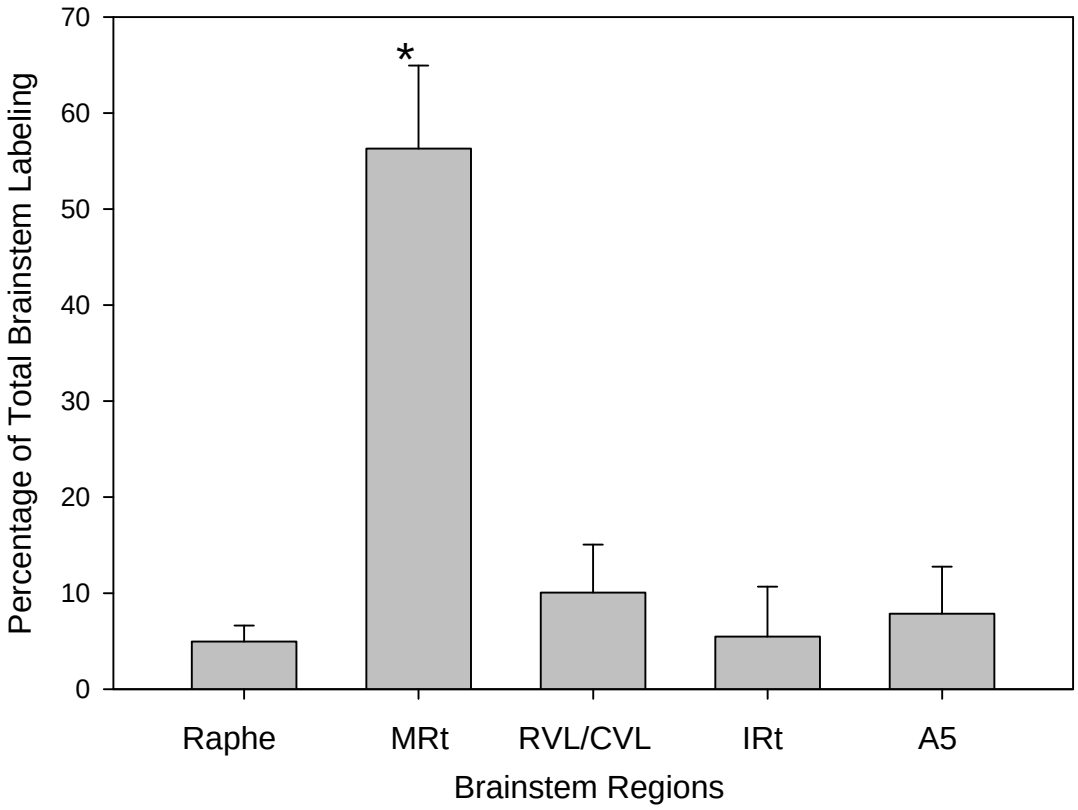

Figure 3-3: 56 hours uninjured – most labeled brainstem regions

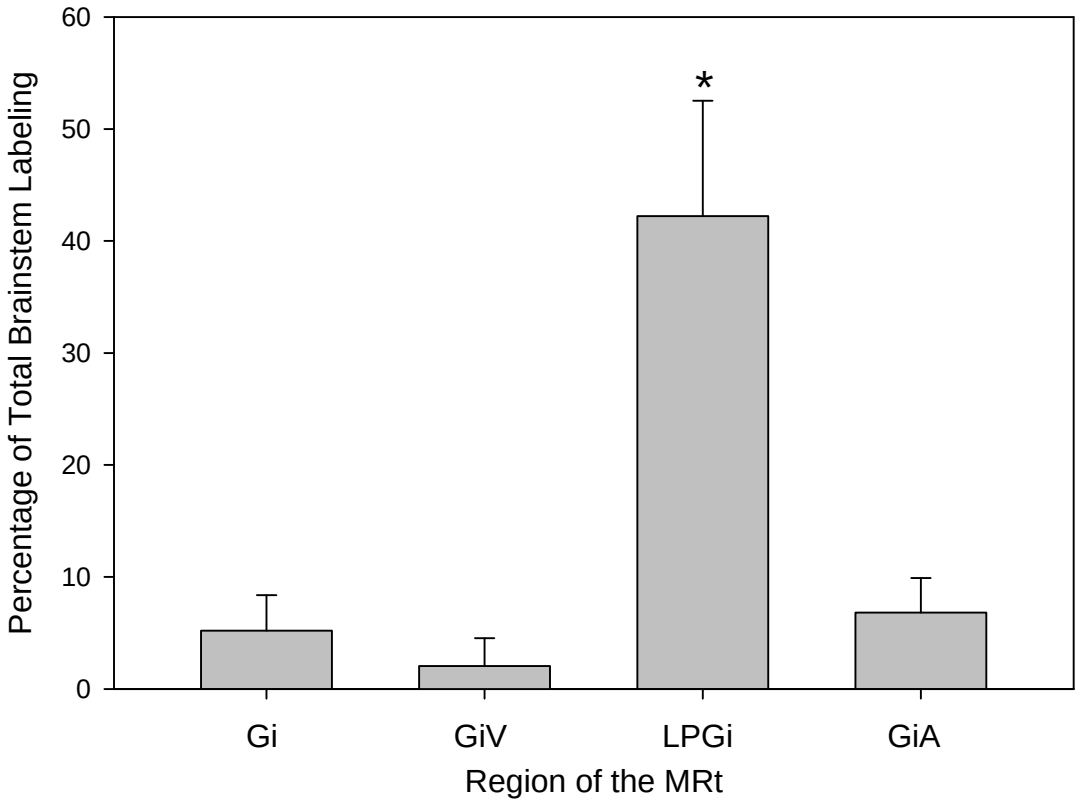

Figure 3-4: 56 hours uninjured – regions of the MRt

Table 3-2: Percentage of total labeling in brainstem in each region at 64 hours

	Region	Mean	SE
Overall brainstem	MRt	42.37	2.26
	RVL/CVL	12.95	0.52
	Raphe	8.64	2.07
	A5	7.40	2.05
	SubC	4.97	1.08
	rVRG	4.97	2.87
Regions of MRt	LPGi	31.43	2.72
	GiA	4.92	1.24
	GiV	3.19	1.25
	Gi	2.29	0.33
	DPGi	0.53	0.17

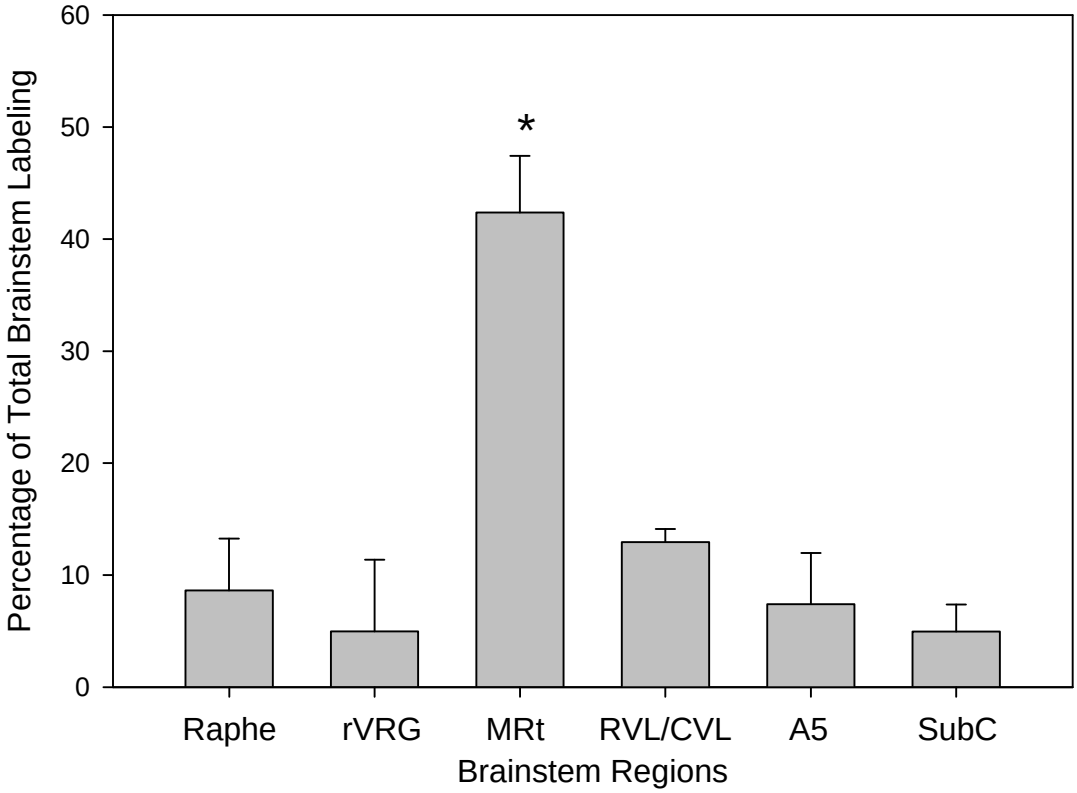

Figure 3-5: 64 hours uninjured – most labeled brainstem regions

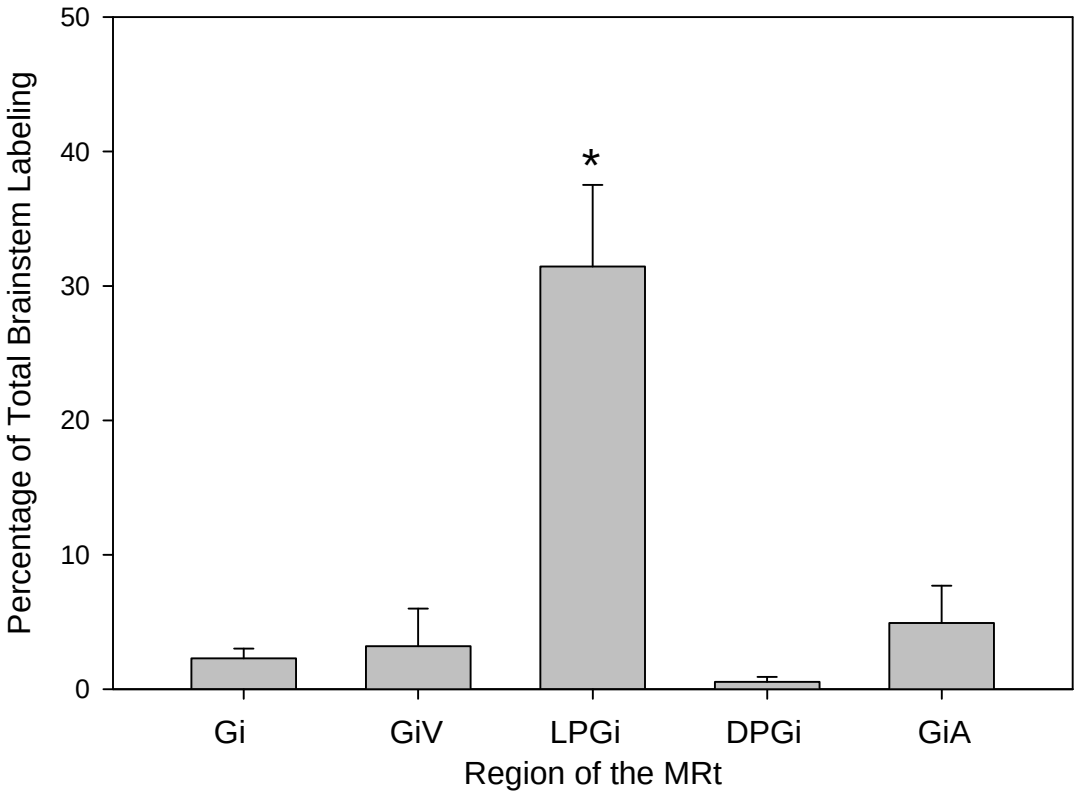

Figure 3-6: 64 hours uninjured – regions of the MRt

Table 3-3: Total number of labeled cells in each side of the brainstem per animal at 64 hours post-infection

	Animal	Left	Right
Uninjured	1	113	132
	2	272	213
	3	703	501
	4	285	286
	5	507	364
Injured	6	166	1562
	7	25	202
	8	23	360
	9	10	101

Table 3-4: Mean percentage of labeling in brainstem in each region at 64 hours (left side/right side)

	Raphe	rVRG	Gi	RVL/CV	IRt	A5	SubC
Uninjured	11.90/8.51	5.02/5.15	45.39/40.48	14.07/12.21	3.40/4.18	6.16/8.90	5.91/3.18
Injured	16.31/12.83	3.74/0.90	44.67/48.11	4.65/7.39	5.74/0.88	6.94/9.18	3.6/2.19

Note: The standard errors are as follows: Uninjured left side = 4.91, Injured left side = 5.49, Uninjured right side = 3.07, Injured right side = 3.43.

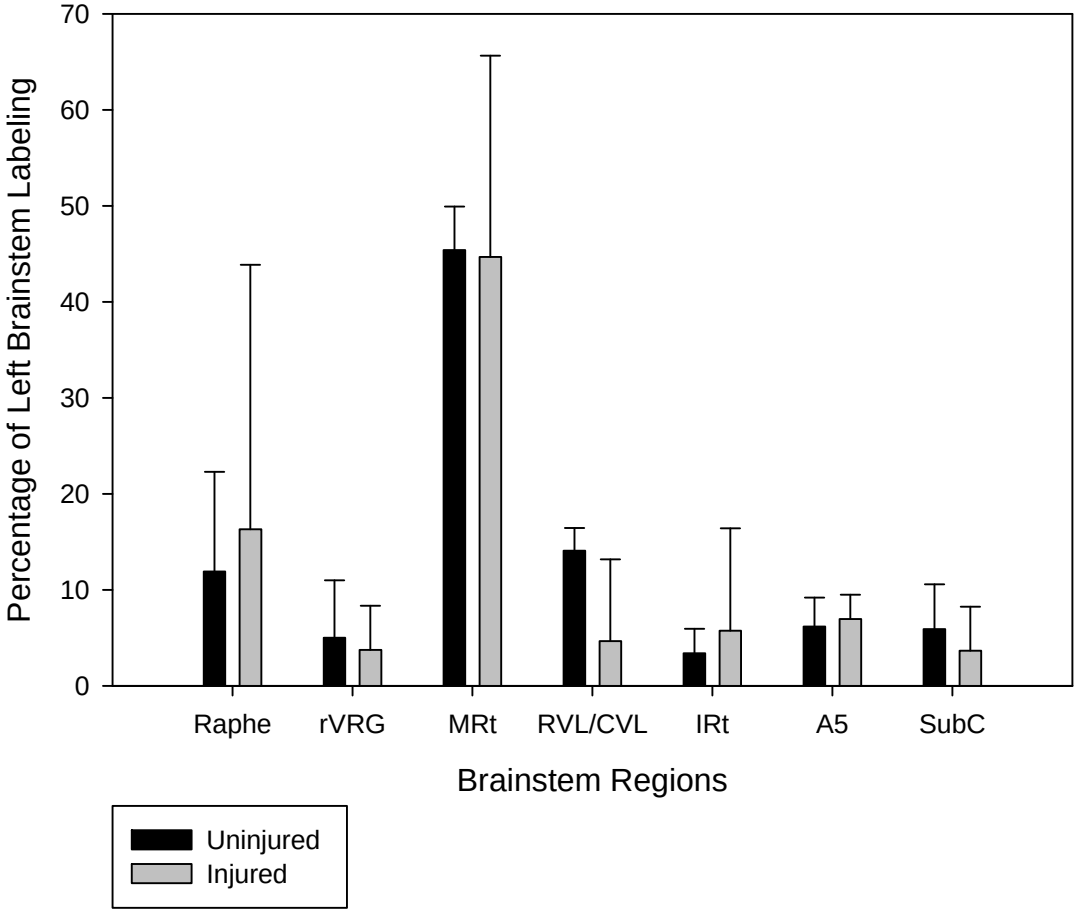

Figure 3-7: 64 hours uninjured and injured – percent of total labeling on left brainstem

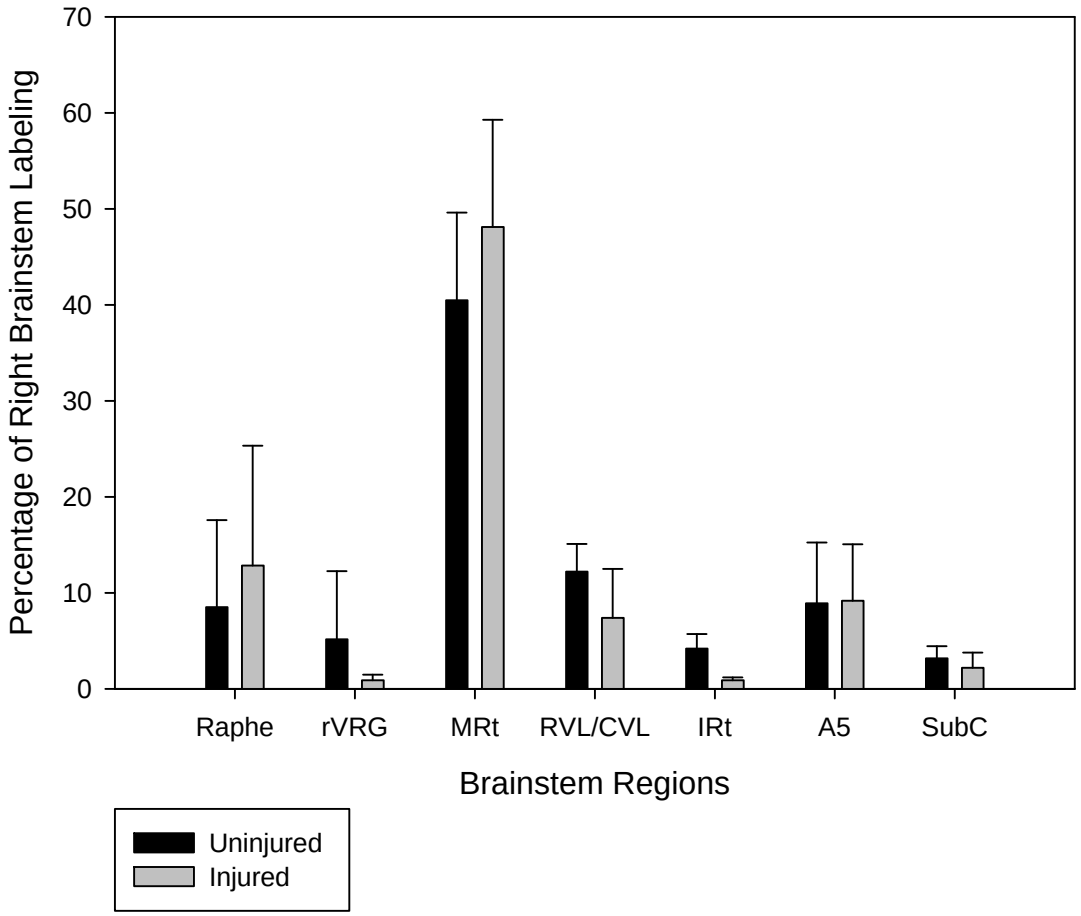

Figure 3-8: 64 hours uninjured and injured – percent of total labeling on right brainstem

CHAPTER 4
DISCUSSION

This study represents the first attempt to quantitatively determine the regional distribution of medullary neurons projecting to PhMNs in both the normal and SCI-injured rat. These initial results suggest that despite unilateral denervation of the PRV-infected phrenic nucleus, which caused reduced labeling in the ipsilateral brainstem, the bilateral pattern and relative proportion of infected brainstem neurons was comparable to observations and data in normal animals. In addition, while the rVRG is considered to be the primary source of inspiratory drive to PhMNs, it quantitatively exhibited far less extensive labeling by transneuronal PRV in normal and injured animals than other regions of the medulla. In fact, the most significant second-order brainstem labeling was in the MRt, the role of which in respiratory control is not entirely clear. Before discussing the implications of these findings relative to normal and post-SCI respiratory function, it is first necessary to address several technical considerations concerning the methods employed in the present study.

Technical Considerations

Pseudorabies Virus as a Retrograde Transynaptic Tracer

For many reasons, the decision to use PRV as the neuroanatomical tracer in the present study was motivated by a previous report in which monosynaptic tracers were used to evaluate rVRG projections to PhMNs after a C2 hemisection (Boulenguez et al., 2007). Neurotropic viruses, such as PRV, are effective as transneuronal tracers that can define a pathway of cells which are synaptically connected. Viruses in general are well suited for neuroanatomical tracing because they can produce controlled viral infections that traverse multiple synapses in sequential order within a network of synaptically linked neurons (Card and Enquist, 1999; Loewy, 1998). This is in contrast to more conventional retrograde tracers (such as FG), which label only a

single cell and never traverse a synapse (Loewy, 1998). Moreover, the fact that PRV can be applied peripherally is especially advantageous because applying the virus to a peripheral nerve or muscle (i.e., the diaphragm) can avoid labeling of cells in the CNS which are not involved in the neuronal circuit of interest. Additionally, these transneuronal tracers move sequentially across synaptic connections in a hierarchical fashion. Thus, temporal analysis can reveal the order of synaptic connectivity (Card and Enquist, 1999; Loewy, 1998).

The strain of PRV used in the present study is PRV-Bartha, which is a naturally occurring attenuated strain of alphaherpesvirus-PRV that has been extremely well characterized in a variety of neuronal networks and has been shown to produce reliable transneuronal infections in a number of species (Card, 1998; Loewy, 1998; Yates et al., 1999). Many characteristics of this strain have made it particularly suitable as a tracer. For instance, the reduced virulence of PRV-Bartha has made it less cytopathogenic to the neurons that it infects (Card, 1998). This allows viral infection through a given circuit to be examined over several days before the onset of cell death (Loewy, 1998). Also important is the fact that PRV-Bartha has been repeatedly found to produce viral infections in an exclusively retrograde direction (i.e., from axon terminal to cell body) (Card et al., 1998). Thus, by using PRV-Bartha it is assured that cells in a neuronal circuit are progressively labeled in a specific hierarchical fashion, progressing from axon to soma and from one cell to cells that project directly to that cell.

Additionally, the factors determining the rate of transneuronal labeling have been well-characterized. The time it takes PRV-Bartha to infect neurons in a multisynaptic circuit is predominantly determined by viral titer and the density of innervation (Aston-Jones and Card, 2000; Card et al., 1998; Card et al., 1999). Relative to the latter, neurons that more densely

innervate or show more synaptic connectivity with previously infected cells will show earlier infection (Card et al., 1999).

Thus, the many qualities of PRV-Bartha led to its selection as the tracer employed to examine the brainstem-phrenic circuit in the present study. For the purposes of this study, only second-order brainstem neuronal infections were considered. Because the concentration of virus was held constant, the main determinant of the temporal pattern of second-order infection was the degree of synaptic connectivity to the PhMN pool. In essence, brainstem neurons with dense projections to the PhMNs showed early PRV infection.

Variability and Normalization of Brainstem Cell Counts

In the present study PRV was topically applied to the diaphragm. This method of tracer application was chosen over diaphragm injections to limit the variability in labeling, as the current method has been found to result in more consistent patterns of neuronal infection (unpublished results). Nonetheless, there was substantial variability in the total number of infected neurons between animals at any given post-infection interval. Some of the variability in labeling could be accounted for by incomplete primary labeling of the PhMN pool. Such variability has been described in previous studies (Lane et al., 2008b) and could be a factor in the disparity of higher-order brainstem labeling seen between animals in the current study.

Despite the advantages of PRV, it (like most retrograde tracing methods) is subject to considerable variability. Raw counts of infected cells are thus difficult to compare within and between animal groups. Counts of infected brainstem neurons in uninjured animals were thus normalized as a function of total infected brainstem neurons in each animal. Similarly, in comparing brainstem labeling in uninjured versus C2 hemisected animals, the counts were normalized as a function of total infected neurons on the left and right sides of the brainstem independently in each animal. Unfortunately, as will be explained later, a major limitation in this

normalization arises when comparison is made between injured and uninjured animals. For that reason, interpretations presented below are tentative and based solely on the inherent assumptions of the normalization approach taken. Alternative quantitative strategies will be required in the future to more adequately assess lateralized differences in labeling in the injured circuit.

Pattern of Brainstem Neurons After Spinal Cord Injury

Prevalence of Crossed Projections to PhMNs

When considering spontaneous respiratory neuroplasticity after high cervical hemisection, an important question is whether any demonstrable changes occur in the distribution of brainstem neurons projecting to the denervated PhMN pool. Previously, in a brief study, Moreno et al. (1992) used wheatgerm agglutinin conjugated to horseradish peroxidase (WGA-HRP) to trace the brainstem origin of axons which drive the PhMNs in C2 hemisected rats. Moreno made injections of this retrograde tracer into functionally recovered hemidaphragm muscle and observed that labeled cells were found bilaterally in the rVRG. While no quantification was attempted, this suggested the presence of spinal decussating rVRG axons which originate in both sides of the brainstem and may mediate the CPP.

More recently, Boulenguez et al. (2007) injected FG into the spinal cord in the vicinity of the PhMNs in rats after C2 hemisection and attempted to quantify the brainstem neurons within the rVRG that cross the spinal midline. Their observations indicate that the number of rVRG neurons that became labeled in hemisected animals represented only a small proportion of those labeled in control animals (23% ipsilaterally and 36% contralaterally). The cells labeled after injury represent brainstem neurons with axons that decussate at the level of the PhMNs, which may be involved in the CPP.

However, there are several limitations with the methods employed in the Boulenguez study. For instance, it was clear that the extent of FG labeling was extremely diffuse, because labeled cells were not restricted to PhMNs and were found on the entire left side of the spinal cord. Hence, it was impossible to be certain that the FG-labeling was restricted the phrenic respiratory circuit. Also, while the authors did not quantify the entire column of cells that were labeled in the rVRG, instead only counting cells in a single 30 μm transverse brainstem section per animal, they made quantitative statements regarding the extent of labeling.

In the present study counts were taken of every labeled neuron in consecutive 40 μm brainstem sections. Thus, the current study represents a more holistic profile of the brainstem regions that project to PhMNs than any previous study. It was found from an examination of the raw counts of labeled cells in individual animals that, consistent with Boulenguez et al. (2007), there was less total brainstem labeling ipsilateral to hemisection (Table 3-3). However, in contrast with that study, there did not seem to be a substantial decrease in labeling contralateral to injury (Table 3-3). Because bulbospinal axons which descend the spinal cord ipsilateral to injury are interrupted by hemisection, the subset of neurons labeled in the ipsilateral brainstem must decussate twice: once at the level of the brainstem and again at the level of the PhMNs, while the neurons labeled contralaterally must decussate only once at the level of the PhMNs. Since labeling only appeared to be attenuated ipsilaterally (relative to controls), the current findings suggest that double-decussating neurons may represent a small portion of bulbospinal fibers that contact PhMNs, as was suggested by Boulenguez. But neurons which decussate once at the level of the cervical spinal cord may be more prevalent. However, due to the variability seen in total brainstem labeling between animals, no statistical analyses were performed and

therefore no quantitative statements can be made regarding the extent of spinal decussation in this circuit.

Persistent Regional Brainstem Labeling After Spinal Cord Injury

Additionally, the proportion of regional labeling in the brainstem was examined. Quantitative analyses revealed that at 64 hours post-PRV infection, hemisected animals showed no differences from normal animals in the overall pattern of brainstem labeling. That is, after SCI, the proportions of regional labeling did not significantly differ from those of control animals on either side of the brainstem (Figures 3-7 and 3-8), indicating that the brainstem regions which contact the PhMNs pre-injury are not substantially altered post-injury. Thus, the neurons that remain synaptically linked to the PhMN pool after SCI, and notably those in the MRt, could prove to be important from a therapeutic perspective, as they may be influential in mediating the CPP and could be viable targets for the development of novel methods of breathing augmentation.

Considerations when Interpreting Brainstem Labeling After Spinal Cord Injury

In the current study brainstem labeling was examined at a two weeks post-hemisection interval. The selection of this time point after injury was based upon evidence from several prior studies indicating that two weeks after hemisection is the earliest onset of the spontaneous CPP (Fuller et al., 2008; Fuller et al., 2006; Fuller et al., 2003; Golder and Mitchell, 2005). However, it is important to note that in the C2 hemisected animals no neurophysiological analyses were performed to verify that the CPP was actually present at two weeks post-hemisection because it is presently unknown to what degree PRV infection may alter neuronal activity.

Moreover, when interpreting the findings from the hemisected animals in the current study, it is important to note that the prior usage of PRV as a neuroanatomical tracer in lesioned animals has been relatively limited (Kim et al., 2002). Therefore, the possibility exists that

neurons in an injured circuit may exhibit variability in their susceptibility to viral infection. Similarly, it is possible that after injury, peripheral changes at the level of the diaphragm or remodeling at the neuromuscular junction (i.e., between the diaphragm and the phrenic nerve) (Mantilla and Sieck, 2003) could have altered the uptake of PRV into the respiratory circuit. For these reasons, results in the injured animal must be taken with caution.

Another limitation in the present study is that only one post-infection interval was examined in injured animals. Thus, in future studies it will be necessary to examine labeling at multiple time points after PRV infection. This will give insight into any mechanisms of neuroplasticity which could be manifested as an alteration in the time it takes for the virus to traverse this circuit. Nonetheless, the present work can provide some technical insight into the use of this neuroanatomical tracing method after SCI as a means of studying injury-induced neuroplasticity.

Normal Pattern of Brainstem Neurons

An unexpected finding as part of the analysis of normal and spinal injured animals was that the rVRG was one of the lesser labeled regions of the brainstem. Previous neuroanatomical data using PRV (Dobbins and Feldman, 1994) identified the rVRG as the dominant anatomical projection to the PhMN pool in the normal rat because the largest quantity of PRV-positive neurons in any brainstem region that is known to be inspiratory was found there. However, as described in more detail below, the relatively sparse rVRG labeling observed in the present study calls into question this previous conclusion. Interestingly, the MRt appears to project heavily to the PhMNs, thereby suggesting that these neurons may be important in the rat phrenic respiratory circuit.

Rostral Ventral Respiratory Group Projections to PhMNs

Surprisingly, only sparse labeling was seen in the rVRG throughout the time course of PRV infection. Indeed, at the 56 hour time point, the rVRG contained less than 5% of the overall labeling, and at the 64 hour time point, it contained barely 5%, and it was outranked by the MRt, the RVL/CVL, the Raphe, and the A5 (Table 3-2 and Figure 3-5). Therefore, based on the manner in which PRV traverses a multisynaptic circuit, the present results suggest that the rVRG exhibits a relatively lesser degree of connectivity to PhMNs than numerous other brainstem regions.

This observation contrasts with a previous study by Dobbins and Feldman (1994) which concluded that monosynaptic projections from the rVRG in the uninjured rat must represent the dominant anatomical pathway to the PhMNs. This conclusion was made because the largest quantity of PRV-positive neurons in any brainstem region that is known to be inspiratory was found in the rVRG (Dobbins and Feldman, 1994) and because it has been extensively shown that rhythmic inspiratory drive comes from this medullary region (Feldman, 1986). However, examination of representative reconstructions of transverse sections through the brainstem in that study revealed substantial labeling in areas outside of the rVRG (notably within the Gi and GiA) that was not quantified because these areas were not within a known inspiratory region of the medulla (Dobbins and Feldman, 1994). Thus, it is likely that if counts were taken of all labeled brainstem neurons (as was done in the present study), the rVRG would not have represented such a large proportion of labeled cells.

Also, when interpreting the present observation of sparse rVRG labeling, it is important to note that Dobbins and Feldman (1994) injected PRV into the phrenic nerve, in contrast to the current method of topical application of PRV to the diaphragm. Thus, different methods of tracer application may have produced differences in the time required for the virus to infect the circuit

between the studies. For instance, it is possible that if animals in the current study were allowed to survive to a more delayed post-infection interval, the proportion of labeling in the rVRG would increase to reflect the predominant labeling observed by Dobbins and Feldman. However, in the current study particular attention was paid to the identification of the brainstem areas that exhibit the greatest degree of synaptic connectivity to the PhMN pool, and therefore the focus remained on the brainstem areas which showed the earliest infection (i.e., the MRt).

Medial Reticular Formation Projections to PhMNs

Unexpectedly, it was found that the MRt, which is not thought of as a respiratory region of the brainstem, accounted for most of the PRV labeling seen in the brainstem even at the earliest time points examined. It was found that in uninjured animals at both the 56 and 64 hour post-infection intervals, the MRt was the only medullary region that exhibited significantly more labeling than any other region (Figures 3-3 and 3-5). Moreover, examination of the mean percentages in the brainstem regions with the most labeling at both time points shows that the proportion of total brainstem labeling observed in the MRt was several times that of the region with the next highest percentage, typically accounting for nearly half of all PRV labeled cells in the brainstem (Tables 3-1 and 3-2).

The fact that such a large proportion of PRV-labeled cells were consistently found in the MRt suggests that this region contains neurons which project heavily to the PhMN pool. In particular, the LPGi was the only subdivision within the MRt that exhibited significantly more labeling than any of the others, and this persisted at both post-infection intervals (Figures 3-4 and 3-6). Likewise the means show that the proportion of labeling occurring in the LPGi was vastly greater than the region with the next highest percentage and accounted for the majority of labeling that was seen in the MRt (Tables 3-1 and 3-2). Thus, this subdivision of the MRt represents a dominant synaptic projection to the PhMN pool. Interestingly, in both the MRt and

LPGi, there were no significant differences in the proportion of labeling occurring in the left and right sides of the brainstem, indicating that in the normal animal these brainstem cells have bilaterally equivalent degrees of PhMN connectivity.

Previous Evidence for Importance of the Medial Reticular Formation in the Phrenic Respiratory Circuit

This study represents the first neuroanatomical evidence to suggest the importance of the MRt in the phrenic respiratory circuit of the rat. However, this finding is not entirely unprecedented. Indeed, although previous studies using a rat model have almost universally identified the rVRG as the dominant area in the respiratory circuit (Dobbins and Feldman, 1994; Boulenguez, 2007; Feldman, 1986), the fact that the involvement of the MRt in the phrenic respiratory circuit has not been documented may reflect a bias in the literature concerning where inspiratory cells are presumed to be located.

However, studies in species such as the cat and the ferret have indicated that there are likely to be cells other than the rVRG which are important in control of inspiration and PhMN excitability. For instance, the current finding that neurons in the MRt represent the majority of brainstem neurons infected by PRV application to the diaphragm mirrors findings in the ferret (Yates et al., 1999; Billig et al., 2000). Additionally, neurophysiological data in the cat has suggested that there are neurons in the MRt that can be recruited to function as respiratory neurons (Gordievskaya and Kireeva, 1999). However, until now it has been assumed that the presence of functionally important respiratory-related cells in other areas of the brainstem is a characteristic exclusive to emetic species (i.e., species capable of vomiting), unlike the rat (Yates et al., 1999). This is because previous accounts in the rat have largely ignored phrenic-associated labeling in these brainstem areas. Thus, it was assumed that in the ferret the MRt must be important in controlling PhMN excitability during activities which are not exhibited in rats (i.e.,

vomiting) (Yates et al., 1999; Dobbins and Feldman, 1994). As a result, the anatomical importance of respiratory-related neurons in reticular areas of the brainstem has not been extensively examined in the rat. However, the predominant connectivity of the MRt to PhMNs, both before and after SCI, demonstrates that the MRt may play a more important role in respiration in the rat than previously thought.

Moreover, previous neuroanatomical studies in the rat have even suggested the possible presence of a widespread network of brainstem neurons that form connections with PhMNs outside of the rVRG. For instance, labeling similar to that in the present study (Figure 3-2) was seen within the MRt after the injection of a monosynaptic tracer into the region of the PhMNs in rats (Boulenguez et al., 2007). However, such labeling was dismissed as spurious due to the diffuse nature of their CNS injection of tracer. Similarly, evidence from Dobbins and Feldman (1994) using PRV revealed projections from the MRt to PhMNs and documents labeling at early post-infection intervals in regions of the MRt, including the Gi and GiA. However, because Dobbins and Feldman did not feel that these cells represented a respiratory population of cells, they provided no quantification within the MRt. Thus, the predominance of the connections between the MRt and PhMNs in the rat was not appreciated.

Functional Implications of the Medial Reticular Formation in Respiration

Numerous studies in a variety of species have suggested that neurons in the MRt are likely to be functionally involved in respiration. For instance, there have been accounts indicating that these cells may be involved in the coordination of the contractions of respiratory muscles. In fact, it has previously been found in the ferret that neurons in this region of the brainstem provide input to both inspiratory and expiratory motoneurons in the spinal cord, which control the diaphragm and the rectus abdominus muscle, respectively (Billing et al., 2000). From this finding and subsequent neurophysiological examination of cells in this region, it was postulated

that at least a subset of these neurons may be involved in coordinating the contraction of several respiratory muscles to augment breath (Billig et al., 2000; Shintani et al., 2003).

Similarly, cells in the MRt are known to be directly involved in vomiting. Indeed, Miller et al. (1996) concluded that if the MRt is inhibited, then cats are no longer able to vomit. Interestingly, neurons in the rVRG are inhibited during vomiting in the cat, indicating that neurons in this region are not essential for relaying signals during this activity (Yates et al., 1999). Although it is known that rats do not possess the ability to vomit, during this behavior breathing becomes labored. Therefore, it is possible that the MRt neurons are more important in modulating PhMN activity during labored breathing, whereas rhythmicity of breathing (generated by the rVRG) is not as necessary during such behaviors.

Additionally, there are activities that rats do engage in, which require altered patterns of respiration and have been shown to involve MRt neurons. For instance, during rapid eye movement (REM) sleep, breathing becomes more rapid and variable and firing rates of neurons in the MRt increase (Bellingham and Funk, 2000). This suggests that in the rat the function of the MRt neurons may be related to generating patterns of breathing which deviate from passive eupnea (i.e., normal, relaxed breathing).

Moreover, some authors believe that the number of respiratory-related neurons in the reticular formation can increase under conditions where respiration becomes laborious or hindered (Gordievskaya and Kireeva, 1999), such as after a cervical SCI. Thus, it seems especially likely that the MRt's role in both vomiting and REM sleep could be related to the need for augmenting breathing during these behaviors. If this is the case, the MRt may prove to be important in regulating breathing after a cervical SCI, when patients must exert more voluntary control to increase respiration. Supporting this is the fact that the MRt is known to receive input

from the motor cortex in cats, a region largely responsible for volitional movement (Canedo, 1997). Thus, the MRt in the rat may also be involved in volitional control of the diaphragm, possibly coordinating diaphragm adjustments before voluntary movement or when breathing becomes labored.

Therefore, drawing from evidence in a variety of species, it is likely that the MRt is functionally involved in augmenting breath. With this possibility mind, the current finding that the MRt is dominantly connected to PhMNs and that this extensive connectivity persists after a C2 hemisection seems logical. Since after this type of injury breathing becomes laborious, these neurons could become particularly important after such an injury. Thus, these cells could represent a viable target for future investigations into therapeutic methods of improving respiration after SCI.

For this reason, further studies are needed to examine the functional role of these neurons to assess their role in the CPP and respiration generally. In particular, it would be interesting to examine the neurochemical profile of these neurons and whether the activity or firing pattern of the neurons in the MRt are significantly altered after SCI, as this knowledge could provide further insight into possible mechanisms of respiratory neuroplasticity after a cervical SCI. For instance, it would be interesting to find out if cells in the MRt which synapse on PhMNs are serotonergic, since serotonin is known to be important in the modulation of respiratory drive in both the brainstem and PhMNs (Bonham, 1995; Golder et al., 2001a; Goshgarian, 2003) and in the activation of the CPP (Zhou and Goshgarian, 2000).

Additionally, the involvement of the MRt in the phrenic respiratory circuit in the rat and in emetic species such as the ferret suggests that there may be fewer differences in the neurocircuitry between species than it has previously been thought. If this is the case, the rat may

represent an even more practical translational model for investigations involving the CPP as an instance of respiratory neuroplasticity.

Summary

To summarize, the present study represents the first attempt to quantitatively determine the distribution of brainstem neurons projecting to PhMNs in both the normal and C2 hemisected rat. These results suggest that despite unilateral denervation of the PhMNs, the bilateral pattern of infected brainstem neurons is largely unaltered from that of normal animals. In addition, while the rVRG is considered to be the primary source of inspiratory drive to PhMNs, sparse transneuronal labeling with PRV was observed. Unexpectedly, the most significant brainstem labeling was in the MRt, which may be involved in augmenting breath. Therefore, future studies should examine the functional role of the MRt in the phrenic respiratory circuit, with the ultimate goal of developing therapeutics to improve respiratory function in patients with high cervical SCI.

APPENDIX
LIST OF SOLUTIONS

Quenching Solution
- 7ml PBS
- 3ml Methanol
- 165ul 30% H_2O_2

Blocking Solution
- 1ml NGS
- 9ml PBS

Primary
- 1ul Anti-PRV (Rb134)
- 200ul NGS
- 30ul Triton X-100
- 9769ul PBS

Secondary
- 50ul Biotinylated Goat anti-Rabbit
- 200ul NGS
- 30ul Triton X-100
- 9720 PBS

ABC Solution
- 9870 PBS
- 50ul Reagent A
- 50ul Reagent B
- 30ul Triton X-100

DAB Solution
- 20ml PBS
- 1 DAB tablet
- 1.5ul 30% H_2O_2

LIST OF REFERENCES

Aston-Jones G, Card PJ. 2000. Use of pseudorabies virus to delineate multisynaptic circuits in brain: opportunities and limitations. Journal of Neuroscience Methods 103: 51-61.

Baker TL, Mitchell GS. 2000. Episodic but not continuous hypoxia elicits long-term facilitation of phrenic motor output in rats. Journal of Physiology 529: 215-219.

Bellingham MC, Funk GD. 2000. Cholinergenic modulation of respiratory brain-stem neurons and its function in sleep-wake state determination. Clinical and Experimental Pharmacology and Physiology 27: 132-137.

Billig I, Foris JM, Enquist LW, Card JP, Yates BJ. 2000. Definition of neuronal circuitry controlling the activity of phrenic and abdominal motoneurons in the ferret using recombinant strains of pseudorabies virus. Journal of Neuroscience 20(19): 7446-7454.

Boulenguez P, Gauthier P, Kasner A. 2007. Respiratory neuron subpopulations and pathways potentially involved in the reactivation of phrenic motoneurons after C2 hemisection. Brain Research 1148: 96-104.

Brown R, DiMarco AF, Hoit JD, Garshick E. 2006. Respiratory dysfunction and management in spinal cord injury. Respiratory Care 5: 853-870.

Canedo A. 1997. Primary motor cortex influences on the descending and ascending systems. Progress in Neurobiology 51: 287-335.

Card PJ. 1998. Practical considerations for the use of pseudorabies virus in transneuronal studies of neural circuitry. Neuroscience and Biobehavioral Reviews 22(6): 685-694.

Card PJ, Enquist LW. 1999. Transneuronal circuit analysis with pseudorabies viruses. Current Protocols in Neuroscience S9:1.5.1-1.5.28.

Card PJ, Enquist LW, Moore RY. 1999. Neuroinvasiveness of pseudorabies virus injected intracerebrally is dependent on viral concentration and terminal field density. Journal of Comparative Neurology 407: 438-452.

Card PJ, Levitt PR, Enquist LW. 1998. Different patterns of neuronal infection after intracerebral injection of two strains of pseudorabies virus. Journal of Virology 72(5): 4434-4441.

Card JP, Rinaman L, Lynn RB, Lee BH, Meade RP, Miselis RR, Enquist LW. 1993. Pseudorabies virus infection of the rat central nervous system: ultrastructural characterization of viral replication, transport, and pathogenesis. Journal of Neuroscience 13(6): 2515-2539.

Coggeshall RE, Lekan HA. 1996. Methods for determining numbers of cells and synapses: a case for more uniform standards of review. Journal of Comparative Neurology 364(1):6-15.

Dobbins EG, Feldman JI. 1994. Brainstem network controlling descending drive to phrenic motoneurons in rat. Journal of Comparative Neurology 347: 64-86.

Ellenberger HH, Feldman JL, Goshgarian HG. 1990. Ventral respiratory group projections to phrenic motoneurons: electron microscopic evidence for monosynaptic connections. Journal of Comparative Neurology 302(4): 707-714.

Feldman JL. 1986. Neurophysiology of breathing in mammals. In: Bloom FE, editor. Handbook of physiology, the nervous system IV: intrinsic regulatory systems of the brain. Bethesda: American Physiological Society. p 463-524.

Forster HV. 2003. Invited review: Plasticity in the control of breathing following sensory denervation. Journal of Applied Physiology 94(2):784-794.

Fuller DD, Doperalski NJ, Dougherty BJ, Sandhu MS, Bolser DC, Reier PJ. 2008. Modest spontaneous recovery of ventilation following chronic high cervical hemisection in rats. Experimental Neurology 211(1): 97-106.

Fuller DD, Golder FJ, Olson EB Jr, Mitchell GS. 2006. Recovery of phrenic activity and ventilation after cervical spinal hemisection in rats. Journal of Applied Physiology 100(3): 800-806.

Fuller DD, Johnson SM, Olson EB Jr, Mitchell GS. 2003. Synaptic pathways to phrenic motoneurons are enhanced by chronic intermittent hypoxia after cervical spinal cord injury. Journal of Neuroscience 23(7): 2993-3000.

Golder FJ, Mitchell GS. 2005. Spinal synaptic enhancement with acute intermittent hypoxia improves respiratory function after chronic cervical spinal cord injury. Journal of Neuroscience 25(11): 2925-2932.

Golder FJ, Reier PJ, Bolser DC. 2001a. Altered respiratory motor drive after spinal cord injury: Supraspinal and bilateral effects of a unilateral lesion. Journal of Neuroscience 21(21): 8680-8689.

Golder FJ, Reier PJ, Davenport PW, Bolser DC. 2001b. Cervical spinal cord injury alters the pattern of breathing in anesthetized rats. Journal of Applied Physiology 91(6): 2451-2458.

Gordievskaya NA, Kireeva N Ya. 1999. Involvement of reticular neurons of the cat medulla oblongata in the integrative activity of the respiratory center. Neuroscience and Behavioral Physiology 29(3): 327-332.

Goshgarian HG. 2003. The crossed phrenic phenomenon: a model for plasticity in the respiratory pathways following spinal cord injury. Journal of Applied Physiology 94: 795-810.

Goshgarian HG, Ellenberger HH, Feldman JL. 1991. Decussation of bulbospinal respiratory axons at the level of the phrenic nuclei in adult rats: a possible substrate for the crossed phrenic phenomenon. Experimental Neurology 111(1):135-139.

Goshgarian HG, Rafols JA. 1981. The phrenic nucleus of the albino rat: a correlative HRP and golgi study. Journal of Comparative Neurology 201(3): 441-456.

Guillery RW. 2002. On counting and counting errors. Journal of Comparative Neurology 447: 1-7.

Jackson AB, Groomes TE. 1994. Incidence of respiratory complications following spinal cord injury. Arch Phys Med Rehabil 75: 270-275.

Johnson RA, Mitchell GS. 2001. P-Chlorophenylalanine eliminates long-term modulation of the exercise ventilatory response in goats. Respiratory Physiology 128: 161-169.

Kim ES, Kim GM, Lu X, Hsu CY. Xu XM. 2002. Neural circuitry of the adult rat central nervous system after spinal cord injury: a study using fast blue and the Bartha strain of pseudorabies virus. Journal of Neurotrauma 19(6): 787-800.

Lane MA, Fuller DD, White TE, Reier PJ. 2008a. Respiratory neuroplasticity and cervical spinal cord injury: translational perspectives. Trends in neuroscience, in press.

Lane MA, White TE, Coutts MA, Jones AL, Sandhu MS, Bloom DC, Bolser DC, Yates BJ, Fuller DD, Reier PJ. 2008b. Journal of Comparative Neurology, in press.

Loewy AD. 1998. Viruses as transneuronal tracers for defining neural circuits. Neuroscience and Biobehavioral Reviews 22(6): 679-684.

Mantilla CB, Sieck GC. 2003. Invited review: Mechanisms underlying motor unit plasticity in the respiratory system. J Appl Physiol 94(3):1230-1241.

Martin PA, Mitchell GS. 1993. Long-term modulation of the exercise ventilatory response in goats. Journal of Physiology 470: 601-617.

Miller AD, Nonaka S, Jakus J, Yates BJ. 1996. Modulation of vomiting by the medullary midline. Brain Research 737: 51-58.

Mitchell GS, Johnson SM. 2003. Invited review: europlasticity in respiratory motor control. Journal of Applied Physiology 94: 358–374.

Moreno DE, Yu XJ, Goshgarian HG. 1992. Identification of the axon pathways which mediate functional recovery of a paralyzed hemidiaphragm following spinal cord hemisection in the adult rat. Experimental Neurology 116(3): 219-228.

Nantwi KD, El-Bohy AA, Schrimsher GW, Reier PJ, Goshgarian H. 1999. Spontaneous functional recovery in a paralyzed hemidiaphragm following upper cervical spinal cord injury in adult rats. Neurorehabilitation and Neural Repair 13: 225-234.

National Spinal Cord Injury Statistical Center. 2006. Spinal cord injury: facts and figures at a glance. Journal of Spinal Cord Medicine 29: 89–90.

Nudo RJ. 2007. Postinfarct cortical plasticity and behavioral recovery. Stroke 38(2): 840-845.

Paxinos G, Watson C. 1997. The rat brain in sterotaxic coordinates (compact 3rd ed.). San Diego: Academic Press, Inc.

Porter WT. 1895. The path of the respiratory impulse from the bulb to the phrenic nuclei. Journal of Physiology 17:455-485.

Shintani T, Mori RL, Yates BJ. 2003. Locations of neurons with respiratory-related activity in the ferret brainstem. Brain Research 974: 236-242.

Yates BJ, Smail JA, Stocker SD, Card JP. 1999. Transneuronal tracing of neural pathways controlling activity of diaphragm motoneurons in the ferret. Neuroscience 90(4): 1501-1513.

Zhou SY, Goshgarian HG. 2000. 5-Hydroxytryptophan-induced respiratory recovery after cervical spinal cord hemisection in rats. Journal of Applied Physiology 89:1528–1536.

BIOGRAPHICAL SKETCH

Marcella Angelique Coutts was born in Miami, Florida in 1984. She graduated cum laude from the University of Miami in 2006 with dual degrees: A Bachelor of Arts in psychology with a minor in chemistry, and a Bachelor of Health Science in pre-pharmacy studies with a minor in Spanish. Upon entering the University of Florida Interdisciplinary Program in biomedical science in Fall 2006, Marcella was awarded the Alumni Fellowship. Marcella will begin medical school in Fall 2008.